Journal of Applied and Computational Mechanics, Vol. 1, No. 4, (2015), 168-180
DOI: 10.22055/jacm.2015.11237

Journal of
Applied and Computational Mechanics

Local and Global Approaches to Fracture Mechanics Using Isogeometric Analysis Method

Abdolghafour Khademalrsoul[1], Reza Naderi [2]

[1] Assistant professor, Department of Civil Engineering, Shahid Chamran University of Ahvaz
Ahvaz, Iran, ag.khadem@yahoo.com,
[2] Associate professor, Faculty of Civil Engineering, Shahroud University of Technology
Shahroud, Iran, rz_naderi@yahoo.com

Received May 22 2015; revised July 14 2015; accepted for publication July 20 2015.
Corresponding author: Abdolghafour Khademalrsoul, ag.khadem@yahoo.com

Abstract

The present research investigates the implementations of different computational geometry technologies in isogeometric analysis framework for computational fracture mechanics. NURBS and T-splines are two different computational geometry technologies which are studied in this work. Among the features of B-spline basis functions, the possibility of enhancing a B-spline basis with discontinuities by means of knot insertion makes isogeometric analysis method a suitable candidate for modeling discrete cracks. Also, the repetition of two different control points between two patches can create a discontinuity in and demonstrates a singularity in the stiffness matrix. In the case of a pre-defined interface, non-uniform rational B-splines are used to obtain an efficient discretization. T-splines constitute a type of computational geometry technology with the possibility of local refinement and with no topologically rectangular arrangement of control points. Therefore, T-splines can decrease superfluous control points which do not have any major effects on the geometry. Various numerical simulations demonstrate the suitability of the isogeometric approach in fracture mechanics.

Keywords: Fracture mechanics, Isogeometric analysis method, Knot insertion, NURBS, T-spline.

1. Introduction

Problems of fracture mechanics and numerical methods have attracted the attention of many prominent researchers over the years. In addition, the integration between them has been interesting for researchers. Finite element method, meshfree methods and extended finite element method have been used in the computational fracture mechanics context [1-4]. However, material imperfections that arise at the time of production or the use of material are unavoidable, and hence must be taken into account. Therefore, the analysis of a cracked body is highly crucial for engineers. Despite the progress of mesh generators, the initial creation of the mesh with a strong discontinuity remains extremely heavy and difficult [5-7]. On the other hand, with the further development of engineering complex designs, generating exact geometries is also required. We note that a finite element mesh is only an approximation of the CAD (Computer Aided Design) geometry, which we will view as “exact”. This approximation can, in many situations, cause errors in analytical results [8]. Among the various numerical methods, only the isogeometric analysis approach (IGA) which utilizes NURBS as approximation basis functions can create an exact geometry [9, 10]. The major idea in isogeometric analysis is to break down the barrier between engineering design and analysis by reconstituting the entire process [11]. Therefore, using isogeometric analysis in fracture mechanics would be important to have the minimum amount of manipulating in the physical space in the whole of the process.
In fact, the possibility of continuity control in NURBS-based isogeometric analysis becomes the IGA which is a capable approach in fracture mechanics and cohesive zone modeling, alike. Since NURBS-based isogeometric

analysis method possesses unique computational properties, it is possible to create different types of discontinuities by using these facilities. Unlike the partition of unity methods, IGA facilitates the modeling of discrete cracks and cohesive zones without additional evolutions in the physical space or performing a special mathematical formulation in the solution space [12, 13]. Hence, this method of analysis may be attractive for engineers. In fact, the isogeometric analysis method can create the discontinuities through its mathematical abilities. Eventually, these inherent properties of the isogeometric analysis prompted us to use this method in computational fracture mechanics. In this study, both NURBS (Non-Uniform Rational B-splines) and T-splines as two different computational geometry technologies are implemented in the isogeometric analysis framework. Different plates with various predefined edge and center cracks are modeled and the values of stress intensity factors are calculated.

The remainder of this paper is as follows. First, the main topics on isogeometric analysis, NURBS and T-splines are discussed in the rest of Section 1. The principles of fracture mechanics are explained in Section 2. Section 3 introduces the major concept of creating discontinuity in B-splines basis functions. Section 4 introduces the discretization concept in the isogeometric analysis method. The numerical simulations for 2D & 3D problems are studied in Section 5. Discretization of solid using T-splines is examined in Section 6. Finally, conclusions are drawn and summarized in Section 7.

1.1 Isogeometric Analysis Method

The isogeometric analysis method has emerged as an important alternative to traditional engineering design and analysis methods. Isogeometric analysis was introduced in [10] and later described in detail in [9]. In isogeometric analysis, the smooth geometric basis is used as the basis for analysis. Most of the early development in isogeometric analysis focused on establishing the behavior of the smooth NURBS basis in analysis. Research has demonstrated that smoothness offers important computational advantages over standard finite elements [14-16]. Areas of application of isogeometric analysis include turbulence [17-19], fluid-structure interaction [20], structural analysis [15, 16], shape optimization [21, 22]. In reality, the cumbersome and time-consuming process of generation of the finite element mesh vanishes in the isogeometric analysis context. Among the available finite element technologies for capturing discontinuities are interface elements [23, 24] and embedded discontinuities [25, 26]. Nowadays, the partition of unity method (PUM or X-FEM, [27-29]) is regarded as the most flexible element technology for capturing propagating cracks. One application of discretizing the cohesive zone formulation using isogeometric finite elements is to use them in combination with the partition of unity method [1, 2, 30, 31]. In that case, the discontinuities would be embedded in the solution space by means of Heaviside functions. Although such an approach would benefit from both advantages of the isogeometric approach, isogeometric finite elements offer the possibility to directly insert discontinuities in the solutions space. The conceptual idea is that in the isogeometric approach the inter element continuity can be decreased by means of knot insertion, e.g., [16]. In fact, we can create a strong discontinuity or cohesive zone by using inherent specifications of isogeometric analysis method. In addition to increasing the multiplicities of knot values in the parametric space, we can create a strong discontinuity in the physical domain with the repeated control points between two patches with identical coordinates.

1.2 NURBS

In general, B-splines are piecewise polynomials that offer great flexibility and precision for a myriad of modeling applications. They are built from a linear combination of basis functions that span a corresponding B-spline space [10, 11, 32]. These basis functions are locally supported and have continuity properties that follow directly from those of the basis [10]. In particular, conic sections such as circles and ellipses can be precisely constructed by projective transformations of piecewise quadratic curves [8, 33, 34]. NURBS-based isogeometric analysis method can preserve the exact geometry, convenient for free-form surface modeling and has special mathematical properties. NURNS' basis functions can be refined through knot insertion. In actuality, each NURBS of order p is C^{p-1}-continuous. In addition, convex hall and variation diminishing properties are other NURBS mathematical specifications [8, 33]. Consequently, these properties of NURBS have made it interesting for fracture mechanics analysis. A NURBS surface and solid are defined as follows:

$$\mathbf{S}(\xi) = \sum_{\mathbf{i} \in I} \mathbf{P}_{\mathbf{i}} R_{\mathbf{i},\mathbf{p}}(\xi), \tag{1}$$

where $\mathbf{P}_i$ is a set of control points, $R_{\mathbf{i},\mathbf{p}}$ is multivariate basis function and ξ is a parameter value. The corresponding multivariate NURBS basis function is defined as [11]:

$$R_{\mathbf{i},\mathbf{p}}(\boldsymbol{\xi}) = \frac{w_{\mathbf{i}} B_{\mathbf{i},\mathbf{p}}(\boldsymbol{\xi})}{\sum_{\mathbf{j} \in I} w_{\mathbf{j}} B_{\mathbf{j},\mathbf{p}}(\boldsymbol{\xi})}, \tag{2}$$

where $\{w_{\mathbf{i}}\}_{\mathbf{i} \in I}$, is a set of weights and I is the appropriate index set. A multivariate NURBS basis functions are defined using the following relation:

$$B_{\mathbf{i},\mathbf{p}}(\boldsymbol{\xi}) = \prod_{l=1}^{d_p} N^{l}_{il,pl}\left(\boldsymbol{\xi}^{l}\right), \tag{3}$$

where, $d_p = 1, 2, 3, \ldots$ corresponds to the dimension of the problem and *l* must not be confused with the power; hence, this superscript implies any direction in the domain [11, 20].

Univariate B-spline basis functions $N_{i,p}$ are defined recursively by using Cox-de-Boor formula as follow [35, 36]: First, beginning with piecewise constant ($p = 0$), then we have:

$$N_{i,0} = \begin{cases} 1 & \text{if } \xi_i \le \xi < \xi_{i+1}, \\ 0 & \text{Otherwise.} \end{cases} \tag{4}$$

So, for $p = 1, 2, 3, \ldots$ we define the basis functions according to the aforementioned formula as follows:

$$N_{i,p} = \frac{\xi - \xi_i}{\xi_{i+p} - \xi_i} N_{i,p-1}(\xi) + \frac{\xi_{i+p+1} - \xi}{\xi_{i+p+1} - \xi_{i+1}} N_{i+1,p-1}(\xi). \tag{5}$$

Figure 1 shows a NURBS surface and some control points for instance which do not coincide with the surface.

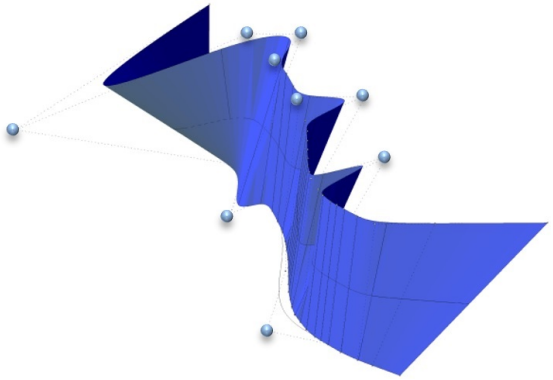

Fig. 1. A NURBS surface, control points are not necessarily coincide the physical domain.

1.3 T-splines

T-splines are introduced after point based splines, or simply PB-splines [37]. Researchers have considered PB-splines to be a suitable alternative to meshless methods [38, 39]. A NURBS surface is defined by using a set of control points, which lie topologically in a rectangular grid. This means that a large number of NURBS control points may be superfluous in that they contain no significant geometric information, but are needed merely to satisfy the topological constraints [11, 32, 38, 40]. T-splines can model complicate designs as a single watertight geometry. Figure 2 shows a gap-free model which is created by means of T-splines in contrast with identical NURBS surfaces [37]. Early studies using T-splines as a basis for isogeometric analysis demonstrated that the T-splines basis possess convergence properties similar to NURBS with far fewer degrees-of-freedom [32]. Additionally, T-splines possess a natural finite element structure which can be integrated seamlessly into existing finite element frameworks via Bézier extraction [32, 39]. As a result, T-splines have been applied to problems in fracture, damage and shells [19].

With NURBS, we used global knot vectors from which all the functions were defined. For T-splines, each function will have its own local knot vector, but these local knot vectors must be inferred from a global structure that encodes a topology and parameterization for the entire T-spline object. This global structure is called the T-mesh. See [37] for more information on how a T-mesh is constructed.

A T-spline is defined in terms of a control grid (or, T-mesh) and global knot vectors $\vec{\mathbf{S}} = [s_{-1}, s_0, s_1, \ldots, s_{c+2}]$ and $\vec{\mathbf{t}} = [t_{-1}, t_0, t_1, \ldots, t_{r+2}]$. Each control point $\mathbf{T}_i$ corresponds to a unique pair of knots (s_j, t_k) and (j, k) will be referred to as the index coordinates of $\mathbf{T}_i$. For each vertex in the T-mesh, a T-spline basis function is constructed, which is called T-spline blending function. There are some discussions on the linear dependency or independency of the blending functions [38]. The T-spline blending functions are defined as follows:

$$\mathbf{T}(s,t) = \frac{\sum_{i=1}^{n_T} \mathbf{T}_i w_i T_i(s,t)}{\sum_{i=1}^{n_T} w_i T_i(s,t)}, \tag{6}$$

where $\mathbf{T}_i = (x_i, y_i, z_i) \in \mathrm{R}^3$ are control points, $w_i \in \mathrm{R}$ are weights, and n_T is the number of control points. $T_i(s,t)$ are blending functions, with

$$T_i(s,t) = B[\vec{\mathbf{s}}_i](s) B[\vec{\mathbf{t}}_i](t), \tag{7}$$

where $B[\vec{\mathbf{s}}_i]$ and $B[\vec{\mathbf{t}}_i]$ are blending functions in *s* and *t* directions, respectively. These two different blending functions are calculated in a manner similar to that of NURBS basis functions, except for the fact that their knot

vectors are local and are inferred from the T-mesh. A T-spline solid and its T-junctions in black circles is shown in Fig. 3.

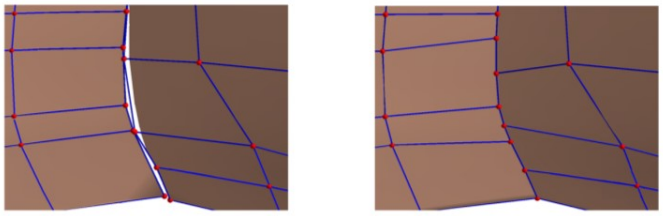

Fig. 2. (Left) Gap and overlapping in NURBS model, (Right) Watertight T-splines

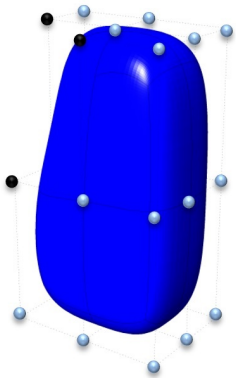

Fig. 3. T-spline solid with T-junctions at upper left corner.

2. Principle of Fracture Mechanics

In fact, the behavior of a body with a discontinuity such as crack and flaw is generally characterized by a single parameter such as stress intensity factors (SIFs) in linear elastic fracture mechanics. Also, throughout the last few decades considerable effort has been put in SIFs calculation. Theoretical, numerical and experimental methods have been employed for the determination of the SIFs in the vicinity of crack tips in cracked bodies. There are three basic modes of deformation according to three independent kinematic movements of upper and lower crack surfaces with respect to each other. Any deformation of crack surfaces can be viewed as a superposition of these basic deformation modes which include opening, sliding and tearing (antiplane) modes. In 2D numerical analysis, we only calculate the two first modes of deformations and the corresponding stress intensity factors.

For two dimensional and any linear elastic body, the crack-tip stress fields are given by a series of the form eq. (8). which is known as Williams' asymptotic solution [56] as follows:

$$\sigma_{ij}(r,\theta) = A_1 r^{-1/2} f_{ij}^{(1)}(\theta) + \mathrm{A}_2 f_{ij}^{(\theta)} + A_3 r^{1/2} f_{ij}^{(3)}(\theta) + \text{higher order terms}, \tag{8}$$

where σ_{ij} is the stress tensor, r and θ are polar coordinates with the origin at the crack-tip. Furthermore, $f_{ij}^{(1)}$, $f_{ij}^{(2)}$, $f_{ij}^{(3)}$ are universal functions of θ, and A_1, A_2, A_3 are parameters proportional to the remotely applied loads. In the vicinity of the crack tip, where ($r \to 0$), the leading term which has the denominator of square-root exhibits singularity. The amplitude of the singular stress fields is characterized by the stress intensity factors (SIFs), i.e. [57, 58]

$$\sigma_{ij} = \frac{K_{\mathrm{I}}}{\sqrt{2\pi r}} f_{ij}^{\mathrm{I}}(\theta) + \frac{K_{\mathrm{II}}}{\sqrt{2\pi r}} f_{ij}^{\mathrm{II}}(\theta), \tag{9}$$

where K_{I} and K_{II} are the mode I and mode II SIFs, respectively. By assuming the small-scale yielding in an elastic body, we can further assume the crack as a semi-infinite domain. Hence, by ignoring the higher order terms in the series the first order equations of the stress fields for mode I are as follows [58]:

$$\begin{bmatrix} \sigma_{xx} \\ \sigma_{yy} \\ \tau_{xy} \end{bmatrix} = \frac{K_{\mathrm{I}}}{\sqrt{2\pi r}} \cos\frac{\theta}{2} \begin{bmatrix} 1 - \sin\frac{\theta}{2}\sin\frac{3\theta}{2} \\ 1 + \sin\frac{\theta}{2}\sin\frac{3\theta}{2} \\ \sin\frac{\theta}{2}\cos\frac{3\theta}{2} \end{bmatrix} \tag{10}$$

2.1 Interaction Integral (*M*-integral)

The interaction integral is derived from the path-independent *J*-integral for two admissible states of a cracked elastic body. As a path independent integral, *J*-integral was originally introduced by J.R. Rice to evaluate strain

concentration by notches and cracks in a linear elastic or non-linear elastic and deformation-type elastic-plastic materials. The *J*-integral is based on an energy balance and is equivalent to the energy release rate during crack extension in a homogeneous elastic body.

The *M*-integral is the dual form of the *J*-integral. The *M*-integral is based on the principle of complementary energy. In effect, the two first values of the stress intensity factors (i.e. K_{I} and K_{II}) could be calculated in one step by utilizing the interaction integral. In addition, the computational efforts may decrease. Consider a 2-D homogeneous crack body of linear or non-linear material free of body forces and tractions on the crack surfaces; the *J*-integral in numerical methods is usually defined as:

$$J = \lim_{\Gamma \to 0} \int_{\Gamma} (W \, \delta_{1j} - \sigma_{ij} u_{i,1}) n_j \, \mathrm{d}\Gamma, \tag{11}$$

where W is the strain energy density given by:

$$W = \int_0^{\varepsilon_{kl}} \sigma_{ij} \, d\varepsilon_{ij} \tag{12}$$

and n_j denotes the outward normal vector to the contour Γ.

We must introduce two admissible states. State 1 ($\sigma_{ij}^{(1)}$, $\varepsilon_{ij}^{(1)}$, $u_i^{(1)}$) corresponds to the actual state and state 2 ($\sigma_{ij}^{(2)}$, $\varepsilon_{ij}^{(2)}$, $u_i^{(2)}$) is an auxiliary state which will be selected as the asymptotic fields for modes I and II. The *J*-integral for the sum of the two states is as follows:

$$J^{(1+2)} = \int_{\Gamma} \left[\frac{1}{2} (\sigma_{ij}^{(1)} + \sigma_{ij}^{(2)})(\varepsilon_{ij}^{(1)} + \varepsilon_{ij}^{(2)}) \delta_{1j} - (\sigma_{ij}^{(1)} + \sigma_{ij}^{(2)}) \frac{\partial (u_i^{(1)} + u_i^{(2)})}{\partial x_1} \right] n_j \, d\Gamma \tag{13}$$

Therefore, by defining the interaction integral, $M^{(1,2)}$, on the equivalent domain of integration and multiplying the integrand by a bounded smoothing function, $q(x)$, that is 1 on an open set containing the crack tip and vanishing on an outer contour, the interaction integral is formulated as follows:

$$M^{(1,2)} = \int_A \left[\sigma_{ij}^{(1)} \frac{\partial u_i^{(2)}}{\partial x_1} + \sigma_{ij}^{(2)} \frac{\partial u_i^{(1)}}{\partial x_1} - W^{(1,2)} \delta_{1j} \right] \frac{\partial q}{\partial x_j} \, dA \tag{14}$$

The interaction integral is calculated by utilizing stress and strains of the Gaussian integration points in the isogeometric analysis framework.

2.2 Cohesive Zone Formulation

Consider a solid $\Omega \subset \mathrm{R}^N \left(N = 2 \text{ or } 3\right)$ as depicted in Fig. 4. The displacement of the material points $x \in \Omega$ is described by the displacement field $u \in \mathrm{R}^N$. The external boundary of the body is composed of a boundary Γ_u on which essential boundary conditions are provided, and a boundary Γ_t with natural boundary conditions. In addition, the internal boundary, Γ_d, is given which represents either an adhesive interface between two separate regions or a cohesive crack. Under the assumption of small displacements and displacement gradients, the deformation of the material is characterized by the infinitesimal strain tensor, $\varepsilon_{ij} = \frac{1}{2}\left(\frac{\partial u_i}{\partial x_j} + \frac{\partial u_j}{\partial x_i} \right)$.

Furthermore, the crack opening $\left[\left| u_i \right|\right]$ is defined as the difference between the displacements on either side of the internal discontinuity Γ_d. In the absence of body forces, the strong form quasi-static equilibrium equations are then given by

$$\begin{cases} \dfrac{\partial \sigma_{ij}}{\partial x_j} = 0 & x \in \Omega \\ u = \hat{u} & x \in \Gamma_u \\ \sigma_{ij} n_j = \hat{t}_i & x \in \Gamma_t \\ \sigma_{ij} n_j = t_i \left(\left[\left| u \right|\right] \right) & x \in \Gamma_d \end{cases} \tag{15}$$

However, the weak form of the equilibrium equations is obtained by multiplication with a virtual displacement δu and integration over the domain Ω. After the application of Gauss' theorem, this results in

$$\int_{\Omega} \sigma_{ij} \, \delta\varepsilon_{ij} \, d\Omega + \int_{\Gamma_d} t_i \, \delta \left[\left| u_i \right|\right] d\Gamma_d = \int_{\Gamma_t} \hat{t}_i \, \delta u_i \, d\Gamma_u \, , \tag{16}$$

where σ is the Cauchy stress tensor and n is the vector normal to the boundaries. Further, the prescribed boundary displacements and tractions are given by $\hat{u}$ and $\hat{t}$, respectively, and the Einstein summation convention is used. From an implementational point of view, it is convenient to rewrite the weak form, eq. (12) in the matrix-vector notation as:

$$\int_{\Omega} \sigma^T \delta\gamma \, d\Omega + \int_{\Gamma_d} \mathbf{t}^T \delta\left[\left|u\right|\right] d\Gamma_d = \int_{\Gamma_t} \hat{\mathbf{t}}^T \delta\mathbf{u} \, d\Gamma_u , \tag{17}$$

where σ and γ are the Voigt form of the Cauchy stress tensor and engineering strain, respectively.

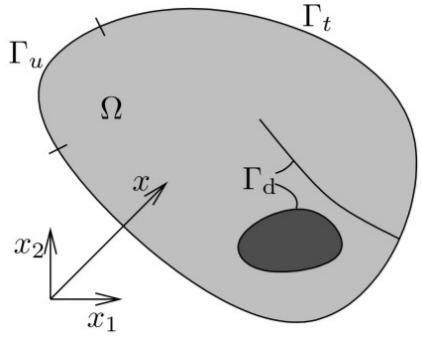

Fig. 4. T-spline solid with T-junctions at upper left corner.

3. Discontinuities in B-splines, NURBS and T-splines

The fundamental building block of isogeometric analysis is the univariate B-spline [8, 34]. A univariate B-spline is a piecewise polynomial defined over a knot vector $\Xi = \left\{\xi_1,\ \xi_2,\ \xi_3,\ \ldots,\ \xi_{n+p+1}\right\}$ where *n* is the number of basis functions and *p* is the polynomial order. As a result, the knots divide the parametric domain $\left[\xi_1,\ \xi_{n+p+1}\right] \subset \mathrm{R}$ into knot intervals of non-negative length. We refer to knot intervals of positive length as elements so we have the knot elements. When several knot values coincide, their multiplicity is indicated by m_i, where i corresponds to the index of the knot values. The B-splines used for analysis purposes are generally open B-splines, which means that the multiplicity of the first and last knots (i.e. m_1 and m_{n+p+1}) are equal to $p+1$. The property of NURBS of particular interest for fracture mechanics is that they are $p - m_i$ times continuously differentiable over a knot i. This allows for the direct discretization of higher-order differential equations [62]. The ability to control inter-element continuity is useful for cohesive zone models since discontinuities can be inserted arbitrarily by means of knot insertion. In fact, a jump in the displacement field at a certain point $x_d = x\left(\xi_d\right)$ in the physical space can be created by raising the multiplicity of the knot ξ_d to $m_i = p+1$.

In general, a function u of several variables (x, y,...) is said to be of class $C^d(\Omega)$ in a domain Ω if all its partial derivatives with respect to (x, y,...) of order up to and including d exist and are continuous in Ω. Thus, if u is of class C^0 in a two dimensional domain Ω, then u is continuous in Ω (i.e., $\partial u/\partial x$ and $\partial u/\partial y$ exist but may not be continuous).

In the current study, a 3D model is created to show the effects of cohesive zone modeling in a NURBS body. In this example, we utilized polynomials of order 3 in both *x* and *y* directions and a polynomial order 2 in *z* direction. This NURBS solid body is comprised of one patch with the size of 5×7×4. The lengths of knot vectors in *x*, *y* and *z* directions are 15, 17 and 8, respectively. The constitutive of material is considered to be linear elastic. The loading condition is uniaxial tension, $\sigma = 1$ which is applied on both sides of the body in *y* direction.

Figure 5 depicts NURBS solid body with a cohesive surface at parametric value of, $\eta = 1/3$, and the distribution of ε_{yy}. In effect, a jump in strain results is obvious; as a result, a global discontinuous surface is created without any manipulation in physical space.

Additionally, we create a discontinuity in a domain with the repetition of different control points between two patches. A singularity occurs in the stiffness matrix due to this procedure and we can capture the effects of a strong discontinuity in the physical space. In contrast to C^0 finite elements, a control point or variable does not generally coincide with an element vertex in the physical space. Furthermore, because the NURBS basis functions do not satisfy the Kronecker delta property, a direct imposition of essential boundary conditions need to utilize a special method [13]. In Fig. 6 we illustrate different methods for the creation of discontinuities in the isogeometric analysis framework. We utilize this procedure to analyze a domain with local strong crack discontinuity such as edge and center cracks.

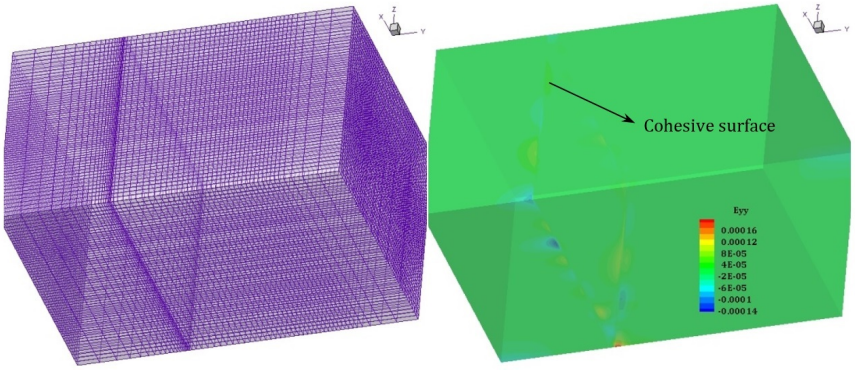

Fig. 5. 3D NURBS solid with a cohesive zone at 1/3 of its height.

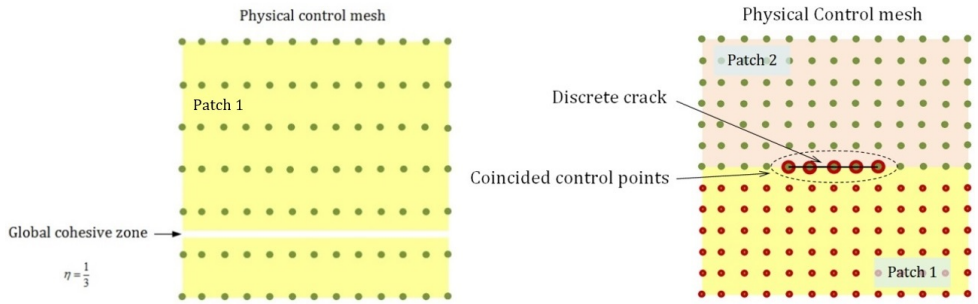

(a) **(b)**

Fig. 6. Discretization approaches in isogeometric analysis for cohesive zone modeling, (a) Global cohesive zone modeling using parametric space, (b) local strong discontinuity modeling using control points.

4. Discretization of a solid with pre-defined discontinuity using NURBS

4.1 Field Parameterization

In this section only the formulation of two dimensional problems is discussed with the aim of alleviating the contents of the paper. NURBS (or B-spline) basis functions are used for both the parameterization of the geometry and the approximation of the solution space for the displacement field $\mathbf{u}$ that is

$$\mathbf{u}(\xi,\eta)=\sum_{i=1}^{n}\sum_{j=1}^{m}R_{i,j}^{p,q}(\xi,\eta)\mathbf{U}_{i,j}, \tag{18}$$

where $R_{i,j}^{p,q}$ are the bivariate NURBS basis functions and $\mathbf{U}_{i,j}$ are the displacement control variables.

4.2 Geometry approximation

The parameterization of a body $\Omega \subset \mathrm{R}^2$ can be obtained by a NURBS surface. Such a surface can comprise one or more NURBS surfaces. A two-dimensional NURBS patch (i.e., any B-spline associated with a particular set of knot vectors, polynomial orders and control points is referred to as a patch) gives a bivariate parameterization of Ω based on the knot vectors $\Xi=\{\xi_1,\xi_2,\xi_3,...,\xi_{n+p+1}\}$, and, $\mathcal{H}=\{\eta_1,\eta_2,\eta_3,...,\eta_{m+q+1}\}$, such that $(\xi,\eta)\in[\xi_1,\xi_{n+p+1}]\otimes[\eta_1,\eta_{m+q+1}]\subset\mathrm{R}^2$.

$$\mathbf{x}(\xi,\eta)=\sum_{i=1}^{n}\sum_{j=1}^{m}R_{i,j}^{p,q}(\xi,\eta)\mathbf{X}_{i,j}, \tag{19}$$

where $\mathbf{X}_{i,j}$ are the coordinates of the control points. It should be noted that when all weights of control points are equal and in the especial form equal to one, NURBS basis functions degenerate to B-spline counterparts. The bivariate and trivariate NURBS basis functions are given by

$$R_{i,j}^{p,q}(\xi,\eta)=\frac{N_{i,p}(\xi)M_{j,q}(\eta)W_{i,j}}{\sum_{i=1}^{n}\sum_{j=1}^{m}N_{i,p}(\xi)M_{j,q}(\eta)W_{i,j}}, \tag{20}$$

where $N_{i,\mathrm{p}}(\xi)$, $M_{j,q}(\eta)$ are univariate B-spline basis functions defined over knot vectors Ξ, $\mathcal{H}$, respectively. The set of control points and associated weights is named control net.

5. Numerical Example using NURBS-based IGA

In this section, NURBS surfaces with predefined strong discontinuity such as edge and center cracks are considered. First, for each plate which is assumed under uniaxial tension, we compare the exact solution and the isogeometric analysis results to show the accuracy of the numerical solutions. All NURBS surfaces are created with polynomial order 3 in both directions. The stress distribution condition is assumed as plane strain and material constitutive is considered to be linear elastic. In addition, the solid NURBS with predefined strong discontinuity is generated.

5.1 Edge-crack model

In the present example a predefined edge crack with the length of 0.5 in a 3×6 plate under uniaxial tension is modeled. This domain is comprised of 1233 control points. In fact, the arrangement of the control points is done in a way that would have the maximum control on the NURBS surface in the vicinity of the crack tip. So, we have the topologically rectangular finer control net around the crack tips. In addition, to increase the precision of the numerical integration, we have used the finer parametric space in the vicinity of the crack tip. Therefore, we have the finer knot spans around the crack tip. Also, the polynomial order 3 is utilized in all geometrical directions with the purpose of capturing the sudden changes in stresses at the crack tip. This example is constructed with two patches, and each patch contains 625 individual control points. Hereupon, the length of each knot vector must be considered to be 29 distinct knot values. All knot vectors are open, so the first and last knot values multiplicities are 4. The constitutive of material is assumed to be linear elastic with the properties of $E = 1.0E6$ and $\nu = 0.3$. Figure 7 illustrates the stress distribution and stress concentration at the crack tip and also the sudden changes that occur in the plate shown below.

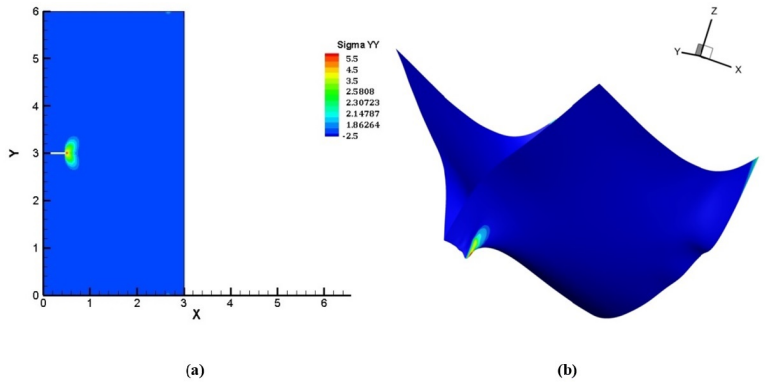

Fig. 7. (a) σ_{yy} distribution in an edge cracked plate, (b) Sudden changes in stress distribution.

In this example a 3D model is generated to show the effects of a discontinuous edge surface in a NURBS solid. The interest domain is created by using 6170 global control points. The arrangement of the control points is chosen in such a way that we have the maximum control on the geometry conditions at the crack surfaces. Hence, the differences between consequent control points decrease gradually till the crack surfaces. This three-dimensional solid NURBS consists of two patches. In all patches the polynomial orders in x and y directions are assumed 3 and in the z direction is considered 2. The loading condition is assumed to be the uniaxial tension which applies in y direction. Figure 8 shows the stress distribution and concentration in two different patches. In order to visualize the discretization of the NURBS volume the physical control mesh is shown.

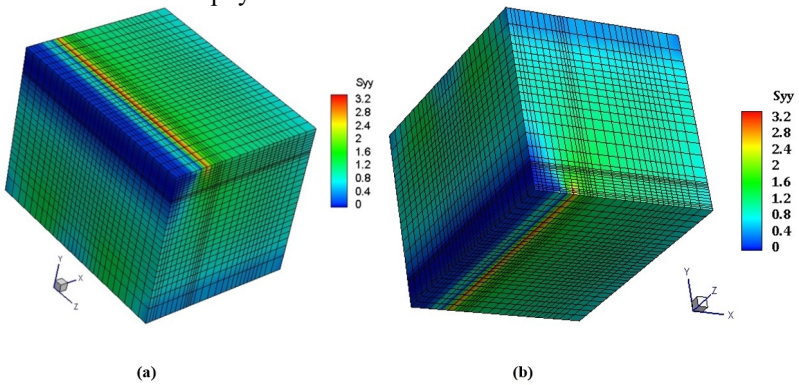

Fig. 8. Three dimensional NURBS volume with predefined edge crack, (a) first patch, (b) second patch.

5.2 Center-crack model

In the following example a predefined center crack with the length of 0.5 in a 3×6 plate under uniaxial tension is modeled. This domain is discretized by using of the 1230 and 4010 physical control points in order to visualize the effects of the control point's pattern. As a matter of fact, the arrangement of the control points is considered in a manner to have the maximum control on the NURBS surface in the vicinity of the crack tips.

So, we have the topologically rectangular finer control net around the crack tips. In addition, we used the finer parametric space in the vicinity of the crack tips to increase the precision of the numerical integration. Therefore, we have the finer knot spans around the crack tips which are assumed to be symmetric for both crack tips. Also, the polynomial order 3 is utilized in all geometrical directions for 2D example with the aim of capturing the sudden changes in the stresses at the crack tips. This example is constructed with two patches, and in two different discretizing schemes, each containing 625 or 2025 individual control points. The arrangements of the control points in two models were chosen 25×25 and 45×45 for each patch. Hereupon, the length of each associated knot vector must be considered to be 29 and 49 distinct knot values for both models. All knot vectors are open, so, the first and last knot values multiplicities are 4. The constitutive of material in the plane strain stress distribution condition is assumed to be linear elastic with the properties of $E = 1.0E6$ and $\nu = 0.3$. Figure 9 illustrates the stress distribution and stress concentration at the crack tips as well as the sudden changes that occur in the plate.

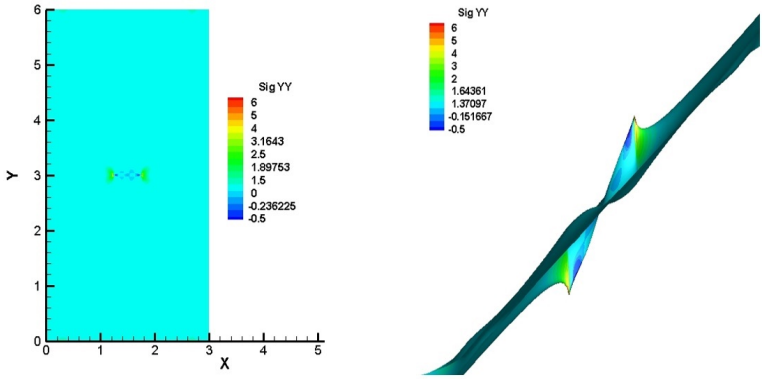

Fig. 9. Isogeometric analysis result of σ_{yy} distribution for center crack example.

In addition, this example is analyzed in a three-dimensional situation. In the case of 3D center discontinuous surface we utilized two patches. The degrees of approximant polynomials are considered to be 3, 3 and 2 in geometrical directions of *x, y* and *z*, respectively. The present 3D NIUBS volume consists of 6150 physical control points in a coordinate in which we have a finer mesh near the crack tip surfaces. Figure 10 shows the three-dimensional NURBS volume with a center crack which is generated by using the repetition of adjacent control points in two patches. In fact in this 3D volume created exactly via NURBS basis functions we found the influences of a discontinuous surface much more easily than other numerical approaches with no excess mathematical computations. However, the simplifications which isogeometric analysis method is induced in the fracture mechanics are utilized. Eventually, we can calculate the main parameter of the linear elastic fracture mechanics such as stress intensity factors easily and preciously.

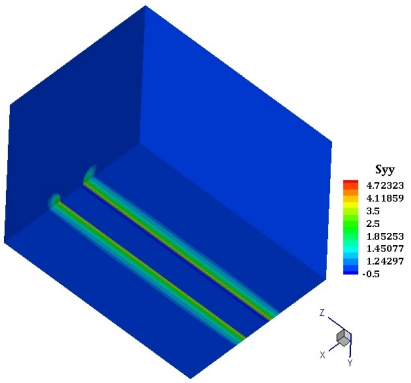

Fig. 10. Three dimensional NURBS volume with a predefined center crack.

5.3 Stress Intensity Factors Calculations

Facture behavior is generally characterized by using a single parameter such as stress intensity factor. There are analytical and experimental solutions for some simple and idealized domain with specific boundary conditions. So, in order to describe the behavior of a cracked body we have to use the numerical methods to calculate fracture parameters. For more information about analytical-experimental solutions see [58, 64, 65]. In this work we attempt to demonstrate the possibility of isogeometric analysis method in the calculation of the fracture mechanic parameters.

So, the values of computational stress intensity factors for mode one and two are compared with the analytical-experimental counterparts. Therefore, in the plane strain condition and for a plate with the width of 3 and height of 6 the values of SIFs are calculated using *J*-integral. This procedure is conducted for the problems of edge crack and center crack. In this comparison the length of each kind of the crack is chosen to be variable. In fact, according to geometry restrictions, the lengths of the crack (i.e. edge or center) are varied from 0.1 to 2.0. Table 1 illustrates the compatibility of the computational and the analytical SIFs which are calculated for a plate with an edge crack. Because the width of the domain is 3, when the edge crack length is 2.0 we have the maximum error in SIFs.

Table 1. Comparison between analytical-experimental values of SIFs and numerical results for edge crack problems.

Crack length	Analytical-experimental K_I	Numerical K_I	Numerical K_{II}	K_I(Numerical)/K_I(Analytical)
0.1	0.6296	0.6251	0.0018	0.993
0.2	0.9082	0.9135	0.0025	1.006
0.3	1.1493	1.1547	0.0032	1.005
0.4	1.3846	1.3869	0.0038	1.001
0.5	1.6266	1.6258	0.0044	0.999
0.6	1.8825	1.8789	0.0051	0.998
0.7	2.1581	2.1535	0.0058	0.998
0.8	2.4591	2.4532	0.0008	0.998
0.9	2.7927	2.7905	0.0009	0.999
1.0	3.1674	3.1708	0.001	1.001
1.5	6.1407	6.1340	0.0161	0.999
2.0	13.1032	13.4695	0.0038	1.028

The same procedure is implemented to calculate the SIFs for the center crack. The horizontal center cracks with different lengths are modeled to examine the capability of the method in fracture mechanics. In fact, having the precise mixed mode stress intensity factors will help us to understand the crack initiation angle to growth accurately. All the present examples are under uniaxial tension loading. According to the geometry configuration and loading conditions, we obtained symmetric results for both crack tips in the domain. The results are listed in Table 2 which shows that the error in estimating SIFs increases slightly as the length of the center crack increases. While the crack tips approach the edges of the domain (i.e., geometrical boundaries), hence, the possibility of the error increases.

Table 2. Comparison between analytical-experimental values of SIFs and numerical results for edge crack problems.

Crack length	Analytical-experimental K_I	Numerical K_I	Numerical K_{II}	K_I(Numerical)/K_I(Analytical)
0.1	0.3979	0.3982	0.0000	1.001
0.2	0.5648	0.5434	0.0000	1.01
0.3	0.6943	0.6787	0.0000	0.976
0.4	0.8050	0.7919	0.0000	0.984
0.5	0.9043	0.8988	0.0000	0.994
0.6	0.9963	0.9810	0.0000	0.985
0.7	1.0838	1.0701	0.0000	0.987
0.8	1.1687	1.1566	0.0000	0.990
0.9	1.2528	1.2422	0.0000	0.992
1.0	1.3375	1.3278	0.0000	0.993
1.5	1.8153	1.7940	0.0000	0.988
2.0	2.4977	2.4517	0.0000	0.982

6. Discretization of a solid with T-splines

Due to some limitations associated with NURBS technology, it is best to use T-splines. In general, the localized basis function inference is the major motivation behind a T-spline. In this section the local approach in T-spline-based isogeometric analysis is briefly discussed. The basis functions, $R_{i,j}^{p,t}$ is completely defined by a set of local knot vectors $\Xi_{i,j} \subset \Xi$ and $\mathcal{H}_{i,j} \subset \mathcal{H}$ of length $p+2$ and $t+2$, respectively. In the case that the orders p and t are odd, to which we will restrict ourselves in this work, the knot vectors associated with the vertex (i, j) in the index space are $\Xi_{i,j} = \left\{\xi_{i-p+1/2}, \ldots, \xi_i, \xi_{i+p+1/2}\right\}$ and $\mathcal{H}_{i,j} = \left\{\eta_{i-t+1/2}, \ldots, \eta_i, \eta_{i+t+1/2}\right\}$. Therefore, the associated T-spline basis functions with can be calculated respect to those local knot vectors in the subsequent relations. Consider (s, t) to be the local coordinates of Gauss point. A numerical subroutine in the computer program returns the values of all basis functions evaluated at the Gauss point as well as the values of the derivatives of all basis functions with respect to *s* and *t* evaluated at the Gauss point. This subroutine computes the value of the i^{th} basis function and its derivatives, where *i* ranges from one to a number of nodes in the domain. In equation 16 the derivatives of T-spline

basis functions are described. It must be noted that, like the NURBS counterparts, the T-spline basis functions are numerically calculated.

$$\frac{\partial N^{(i)}}{\partial s}(s,t)=\frac{W^{(i)}\frac{dS^{(i)}}{ds}(s)T^{(i)}(t)-N^{(i)}(s,t)\sum_{j=1}^{\text{nnode}}W^{(j)}\frac{dS}{ds}(s)T^{(j)}(t)}{\sum_{j=1}^{\text{nnode}}W^{(j)}S^{(j)}(s)T^{(j)}(t)} \tag{21}$$

where the values of $dS^{(i)}/ds(s)$ and $dT^{(i)}/dt(t)$ are calculated by sending the *s*-coordinate of the Gauss point to the subroutine which corresponds to the T-spline basis functions calculation. In this research study, a test example using T-spline is presented. In this example a plate with a hole is created and the stresses are obtained. The plate is an infinite one with a circular hole under constant in-plane tension. Specifically, the plate is subjected to tensile stress σ_t; the radius of the circular hole α is 5 in; the width and thickness of the plate are 40 and 0.1 inches, respectively; the Poisson's ratio ν is 0.3 and the Young's modulus *E* equals 10000 ksi. For simplicity and analysis reasons, the infinite plate is reduced to a finite quarter plate.

Since in a T-spline based isogeometric analysis we need a T-mesh to infer the local knot vectors for every anchor (namely, the control points), the associated T-mesh for aforementioned example is illustrated in Fig. 11. The corresponding T-mesh in the parametric space contains no rectangular topology. The anchors or control points are not in a particularly rectangular arrangement.

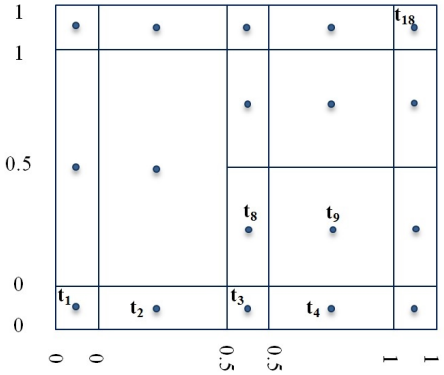

Fig. 11. T-mesh for plate with a hole in the parametric space. Control points are shown in blue solid circles.

Accordingly, the associated basis functions for each control point are calculated via each pair of local knot vectors. For space reasons we briefly describe a specimen for inference of a pair of local knot vectors. Consider control point $\mathbf{t}_8$, the horizontal and vertical local knot vectors to be as follows:

$$\Xi_{\mathbf{t}_8}^{(\text{Horizontal})}=\{0,\,0,\,0,\,0.5\},\ \mathcal{H}_{\mathbf{t}_8}^{(\text{Vertical})}=\{0,\,0,\,0,\,1\}. \tag{22}$$

It should be noted that these knot vectors are for two quadratic polynomials in two directions. Therefore, the length of these knot vectors is 4 (i.e. they contain 4 different knot values). In the present example test, the weight values for the control points $\mathbf{t}_2,\mathbf{t}_3,\mathbf{t}_4$ is 0.85355 and it means that they are in the. The weight of $\mathbf{t}_8,\mathbf{t}_9$ is 0.92678 which means that they are located at 44.12° with respect to the origin in the lower right corner. The weight is calculated by using a relation with respect to the rational Bezier curve generation [8]. Error! Reference source not found.12 shows the stress distribution in the plate with a quarter hole.

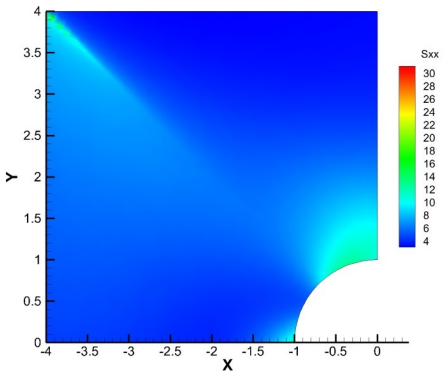

Fig. 12. Stress distribution and concentration in the plate with a quarter hole.

7. Conclusion

In this study, we introduced two different computational geometry technologies and their implementations in both structural analysis and fracture mechanics. NURBS with global and T-splines with local knot vectors are utilized in solving engineering analysis problems. In effect, the same features which make T-splines attractive for design make

it attractive for analysis. T-splines reduce the degree of freedoms in analysis and hence reduce computational efforts. T-splines create watertight surfaces and can be locally refined. The possibility of the local refining of T-splines is shown in the context; however, it is very interesting in the case of the propagating discontinuities. In actuality, the possibility of enhancing a B-spline with knot insertion in the parametric space makes it attractive for creating cohesive zones and strong discontinuity in the physical space without excessive manipulating of the physical domain. Having some specific features, isogeometric analysis has superiority over the partition of unity methods in discontinuity modeling and performing fracture mechanics analysis and design. Furthermore, in isogeometric analysis there are no numerical errors in geometry generating and engineering designs are created with high precision. In fact, expressions of the well-known h, p and hp refinement in FEM are easily handled in the concept of isogeometric analysis. On the other hand, the level of smoothness in IGA is preferable over other numerical approaches. Finally, NURBS and T-splines have the same level of accuracy in analysis; however, T-splines decrease superfluous control points.

Acknowledgments

I would like to thank peer reviewers for their positive comments and my supervisor Dr. Naderi for encouraging me to fulfill this study.

Nomenclature

σ_{ij}	Stress tensor [MPa]	K_I	Stress intensity factor mode 1 [MPa.m$^{1/2}$]
ε_{ij}	Strain tensor	K_{II}	Stress intensity factor mode 2 [MPa.m$^{1/2}$]
W	Strain energy density	$\Xi, \mathcal{H}$	Knot vector
J	Path independent integral	$N_{\mathbf{i,p}}(\xi)$	NURBS basis function
M	Interaction integral	$B_{\mathbf{i,p}}(\xi)$	Multivariate NURBS basis function
E	Modulus of elasticity	$\mathbf{S}(\xi)$	NURBS or T-spline surface
ν	Poisson's ratio	$\mathbf{P_i}$	Control point set
r	r coordinate/ distance from crack tip		
θ	radial angle from crack tip		

References

[1] Bhardwaj G., Singh I.V., Mishra B.K., Bui T.Q., "Numerical simulation of functionally graded cracked plates using NURBS based XIGA under different loads and boundary conditions", Composite Structures, Vol. 126, pp. 347-359, 2015.

[2] Singh I.V., Bhardwaj G., Mishra B.K., "A new criterion for modeling multiple discontinuities passing through an element using XIGA", Journal of Mechanical Science and Technology, Vol. 29, No. 3, pp. 1131-1143, 2015.

[3] Rabczuk T., Belytschko T., Cracking particles: a simplified meshfree method for arbitrary evolving cracks, International Journal for Numerical Methods in Engineering, Vol. 61 No. 13, pp. 2316-2343, 2004.

[4] Naderi R., Khademalrasoul A., "Fully Automatic Crack Propagation Modeling in Interaction with Void and Inclusion without Remeshing" Modares Mechanical Engineering, Vol. 15 No. 7, pp. 261-273, 2015. (In Persian)

[5] Zhuang Z., Liu Z., Cheng B., Liao J., "Chapter 2 - Fundamental Linear Elastic Fracture Mechanics.In": Zhuang Z, Liu Z, Cheng B, Liao J, editors. Extended Finite Element Method. Oxford: Academic Press, pp. 13-31, 2014.

[6] Daxini S.D., Prajapati J.M., "A Review on Recent Contribution of Meshfree Methods to Structure and Fracture Mechanics Applications", The Scientific World Journal, 2014.

[7] Chen T., Xiao Z.-G., Zhao X.-L., Gu X.-L., "A boundary element analysis of fatigue crack growth for welded connections under bending", Engineering Fracture Mechanics, Vol. 98, pp. 44-51, 2013.

[8] Hughes T.J.R., Cottrell J.A., Bazilevs Y., "Isogeometric Analysis Toward integration of CAD and FEM", 2009.

[9] Cottrell J.A., Hughes T.J.R., Bazilevs Y., "Isogeometric Analysis: Toward Integration of CAD and FEA", Wiley, 2009.

[10] Hughes T.J.R., Cottrell J.A., Bazilevs Y., "Isogeometric analysis: CAD, finite elements, NURBS, exact geometry and mesh refinement, Computer Methods in Applied Mechanics and Engineering, Vol. 194, No. 39–41, pp. 4135-4195, 2005.

[11] Bazilevs Y., Calo V.M., Cottrell J.A., Evans J.A., Hughes T.J.R., Lipton S., et al., "Isogeometric analysis using T-splines", Computer Methods in Applied Mechanics and Engineering, Vol. 199, No. 5–8, pp. 229-263, 2010.

[12] Ghorashi S.S., Valizadeh N., Mohammadi S., "Extended isogeometric analysis for simulation of stationary and propagating cracks", International Journal for Numerical Methods in Engineering, Vol. 89, No. 9, pp. 1069-1101, 2012.

[13] De Luycker E., Benson D.J., Belytschko T., Bazilevs Y., Hsu M.C., "X-FEM in isogeometric analysis for linear fracture mechanics", International Journal for Numerical Methods in Engineering, Vol. 87, No. 6, pp. 541-565, 2011.

[14] Evans J.A., Bazilevs Y., Babuška I., Hughes T.J.R., "n-Widths, sup–infs, and optimality ratios for the k-version of the isogeometric finite element method", Computer Methods in Applied Mechanics and Engineering, Vol. 198 No. 21–26, pp. 1726-1741, 2009.
[15] Cottrell J.A., Hughes T.J.R., Reali A., "Studies of refinement and continuity in isogeometric structural analysis", Computer Methods in Applied Mechanics and Engineering, Vol. 196, No. 41–44, pp. 4160-4183, 2007.
[16] Cottrell J.A., Reali A., Bazilevs Y., Hughes T.J.R., "Isogeometric analysis of structural vibrations, Computer Methods in Applied", Mechanics and Engineering, Vol. 195, No. 41–43, pp. 5257-5296, 2006.
[17] Akkerman I., Bazilevs Y., Kees C.E., Farthing M.W., "Isogeometric analysis of free-surface flow", Journal of Computational Physics, Vol. 230, No. 11, pp. 4137-4152, 2011.
[18] Bazilevs Y., Akkerman I., "Large eddy simulation of turbulent Taylor–Couette flow using isogeometric analysis and the residual-based variational multiscale method", Journal of Computational Physics, Vol. 229, No. 9, pp. 3402-3414, 2010.
[19] Bazilevs Y., Calo V.M., Cottrell J.A., Hughes T.J.R., Reali A., Scovazzi G., "Variational multiscale residual-based turbulence modeling for large eddy simulation of incompressible flows", Computer Methods in Applied Mechanics and Engineering, Vol. 197, No. 1–4, pp. 173-201, 2007.
[20] Bazilevs Y., Hsu M.C., Scott M.A., "Isogeometric fluid–structure interaction analysis with emphasis on non-matching discretizations, and with application to wind turbines", Computer Methods in Applied Mechanics and Engineering, Vol. 249–252, pp. 28-41, 2012.
[21] Li K., Qian X., "Isogeometric analysis and shape optimization via boundary integral", Computer-Aided Design, Vol. 43, No. 11, pp. 1427-1437, 2011.
[22] Hassani B., Tavakkoli S.M., Moghadam N.Z., "Application of isogeometric analysis in structural shape optimization", Scientia Iranica, Vol. 18, No. 4, pp. 846-852, 2011.
[23] Rots J., "Smeared and discrete representations of localized fracture", International Journal of Fracture, Vol. 51, No. 1, pp. 45-59, 1991.
[24] Schellekens J.C.J., De Borst R., "On the numerical integration of interface elements", International Journal for Numerical Methods in Engineering, Vol. 36, No. 1, pp. 43-66, 1993.
[25] Simo J.C., Oliver J., Armero F., "An analysis of strong discontinuities induced by strain-softening in rate-independent inelastic solids", Computational Mechanics, Vol. 12, No. 5, pp. 277-296, 1993.
[26] Oliver J., "Modelling strong discontinuities in solid mechanics via strain softening constitutive equations. Part 2: numerical simulation", International Journal for Numerical Methods in Engineering, Vol. 39, No. 21, pp. 3601-3623, 1996.
[27] Belytschko T., Black T., "Elastic crack growth in finite elements with minimal remeshing", International Journal for Numerical Methods in Engineering, Vol. 45, No. 5, pp. 601-620, 1999.
[28] Babuška I., Zhang Z., "The partition of unity method for the elastically supported beam", Computer Methods in Applied Mechanics and Engineering, Vol. 152, No. 1–2, pp. 1-18, 1998.
[29] Babuska I., Melenk, J, "The Partition of unity method", International Journal for Numerical Methods in Engineering, Vol. 40, pp. 727–758, 1997.
[30] Bhardwaj G., Singh I.V., Mishra B.K., "Stochastic fatigue crack growth simulation of interfacial crack in bi-layered FGMs using XIGA", Computer Methods in Applied Mechanics and Engineering, Vol. 284, pp. 186-229, 2015.
[31] Bhardwaj G., Singh I.V., Mishra B.K., Kumar V., "Numerical Simulations of Cracked Plate using XIGA under Different Loads and Boundary Conditions", Mechanics of Advanced Materials and Structures, 2015.
[32] Scott M.A., Li X., Sederberg T.W., Hughes T.J.R., "Local refinement of analysis-suitable T-splines", Computer Methods in Applied Mechanics and Engineering, Vol. 213–216, pp. 206-222, 2012.
[33] Piegl L.A., Tiller W., The Nurbs Book, Springer-Verlag GmbH, 1997.
[34] Rogers D.F., "An introduction to NURBS: with historical perspective", Morgan Kaufmann Publishers, 2001.
[35] De Boor C., "On calculating with B-splines", Journal of Approximation Theory, Vol. 6, No.1, pp. 50-62, 1972.
[36] Cox M.G., "The Numerical Evaluation of B-Splines", IMA Journal of Applied Mathematics, Vol. 10, No. 2, pp. 134-149, 1972.
[37] Sederberg T.W., Zheng J., Bakenov A., Nasri A., T-splines and T-NURCCs, ACM SIGGRAPH 2003 Papers, San Diego, California, 882295: ACM, pp. 477-484, 2003.
[38] Buffa A., Cho D., Sangalli G., "Linear independence of the T-spline blending functions associated with some particular T-meshes", Computer Methods in Applied Mechanics and Engineering, Vol. 199, No. 23–24, pp. 1437-1445, 2010.
[39] Buffa A., Cho D., Kumar M., "Characterization of T-splines with reduced continuity order on T-meshes", Computer Methods in Applied Mechanics and Engineering, Vol. 201–204, pp. 112-126, 2012.
[40] Scott M.A., Simpson R.N., Evans J.A., Lipton S., Bordas S.P.A., Hughes T.J.R., et al., "Isogeometric boundary element analysis using unstructured T-splines", Computer Methods in Applied Mechanics and Engineering, Vol. 254, pp. 197-221, 2013.